Axial invariance of rapidly varying diffusionless motions in the Earth's core interior

Dominique Jault

▶ To cite this version:

HAL Id: hal-00323192

https://hal.archives-ouvertes.fr/hal-00323192

Submitted on 19 Sep 2008

Axial invariance of rapidly varying diffusionless motions in the Earth's core interior

Dominique Jault

LGIT, CNRS, Université Joseph-Fourier, BP 53, 38041 Grenoble Cedex 9, France

Abstract

Geostrophic jets propagating as Alfvén waves are shown to arise in a rapidly rotating spherical shell permeated by a magnetic field among the transient motions set up by an impulsive rotation of the inner core. These axially invariant motions evolve on a time-scale which is short compared to the magnetic diffusion time. The numerical study is taken as illustrative of a more general point: on such a fast time-scale the dimensionless number appropriate to compare the rotation and magnetic forces is independent of the magnetic diffusivity in contrast with the often used Elsasser number. Extension of the analysis to non-axisymmetrical motions is supported by published studies of dynamo models and magnetic instabilities.

Key words: Earth's core, Magneto-hydrodynamic waves, geomagnetic field, core flow

1 Introduction

For the last ten years, numerical simulations of the dynamo process in the Earth's core have much changed the views on the interplay between magnetic and rotation forces. In particular, columnar flows almost invariant in the direction parallel to the rotation axis and localized outside the imaginary cylinder tangent to the inner core have been found very often even though the Elsasser number Λ, classically used to estimate the ratio of magnetic to rotation forces, is of order 1 or larger (see e.g. Olson et al. (1999); Grote and Busse (2001)). Alignment parallel to the rotation axis is caused by the predominance of rotation forces. Accordingly, columnar flows had been contemplated previously

---

in the context of weak-field models ($\Lambda \ll 1$) alone (Busse, 1975). The "strong field regime" ($\Lambda = O(1)$) was illustrated by mean-field dynamo solutions, in which the azimutal angular velocity showed instead large shears in the direction parallel to the rotation axis (Braginsky, 1978; Hollerbach and Jones, 1993; Jault, 1995). These early solutions were either steady or slowly varying on the magnetic diffusion time in sharp contrast with the current generation of dynamo solutions.

With large magnetic fields, as measured by Λ, only the geostrophic part of the velocity field, symmetric about the rotation axis, was expected to be invariant in the direction parallel to the rotation axis. Braginsky (1970) singled out these motions in the context of magnetostrophic equilibrium, characterized by the insignificance of inertial and viscous forces compared to magnetic, rotation and pressure forces. He found that as these azimutal velocities shear the magnetic field, they are subject to a restoring force, provided by the magnetic field, that ensures wave propagation. This is the mechanism of Alfvén waves and indeed geostrophic velocities in a rotating spherical shell permeated by a magnetic field obey an equation of Alfvén wave type save for geometrical factors. Braginsky (1970) assigned these torsional Alfvén waves to perturbations with respect to a slowly evolving basic state characterized by the cancellation of the total action of magnetic forces on the geostrophic cylinders. That description sets the geostrophic velocities apart. My aim, in this paper, is to defend another explanation for the emergence of torsional Alfvén waves that can be generalized to nonaxisymmetric motions, such as the almost axially invariant vortices found in recent geodynamo solutions characterized by strong but rapidly fluctuating magnetic fields. Other examples are outlined in the discussion part.

In the next section, I introduce the two dimensionless numbers Λ and λ that measure the relative strength of the magnetic and rotation forces, within a rapidly rotating body permeated by a magnetic field. I argue that on fast diffusionless time-scales, the appropriate number is λ. This is illustrated in the third section, which constitutes the main body of the article. The competition between magnetic and rotation forces is studied in a rapidly rotating spherical shell immersed in a magnetic field. Specifically, the axisymmetrical transient motions set-up by an impulsive rotation of the inner core are investigated for different values of λ and the Elsasser number. This is followed by a general discussion, where different problems are listed for which λ rather than Λ is appropriate to compare magnetic and rotation forces. The paper ends with concluding remarks.

2   Lehnert versus Elsasser numbers

Elsasser (1946) argued that the magnetic field in the Earth's core saturates when the magnetic force becomes comparable to the Coriolis force and suggested the characteristic strength

$$B = \left(\frac{2\Omega\rho}{\sigma}\right)^{1/2} ,\tag{1}$$

where Ω is the angular velocity, ρ is the density and σ is the electrical conductivity. The Elsasser number,

$$\Lambda = \frac{\sigma B^2}{\Omega\rho} ,\tag{2}$$

has subsequently been used to measure the relative strength of Coriolis and magnetic forces. In order to derive the relationship (1), the electrical current density j is estimated as σUB. This is obviously not valid when magnetic diffusion is negligible compared to induction ($j \ll \sigma UB$).

Conversely, magnetic diffusion does not enter the physics of plane magneto-hydrodynamic waves, of length-scale l that Lehnert (1954) studied. He used another dimensionless number $\chi_0 = \lambda^{-1}$, with

$$\lambda = \frac{B}{\Omega(\mu\rho)^{1/2}l} ,\tag{3}$$

to measure the relative strength of magnetic and rotation forces. The parameter λ, hereinafter referred to as the Lehnert number, can be defined as the ratio, in a rapidly rotating and electrically conducting fluid permeated by a magnetic field, of the period of the inertial waves to the period of the Alfvén waves. Thus, the typical frequency of diffusionless Alfvén waves is $\lambda\Omega$ and the relationship

$$\lambda \ll 1\tag{4}$$

states that rotation forces dominate over magnetic forces on fast time-scales. Cardin et al. (2002) argued that both Λ and λ are important to characterize geodynamo models.

In the spherical case, it is convenient to specify λ using the outer radius a as the length-scale l in the definition (3). Denoting by E_M the magnetic Ekman number $\eta/\Omega a^2$ and by E the ordinary Ekman number $\nu/\Omega a^2$, the relationship,
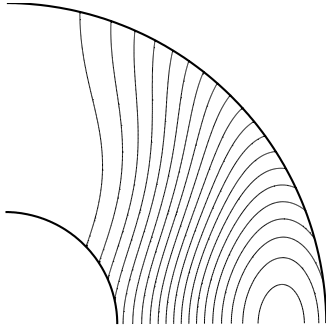
$$E_M + E \ll \lambda,\tag{5}$$

Figure 1. Field lines of the imposed poloidal axisymmetric field.

ensures that Alfvén waves are not rapidly damped by either magnetic or viscous diffusion (ν and η are respectively the viscous and magnetic diffusivities). Indeed, the ratio of λ to $E + E_M$ is the Lundquist number S which indicates how far Alfvén waves propagate before they are quenched by diffusion (Roberts, 1967). The two numbers λ and Λ are related through the magnetic Ekman number:

$$\lambda^2 = \Lambda E_M. \tag{6}$$

The value of λ appropriate to the Earth's core is of the order of $3. \times 10^{-5} - 2. \times 10^{-4}$. Indeed, $\lambda = 10^{-4}$ corresponds to a magnetic field strength in the core interior of the order of 3. mT. Usually quoted values range from 1. mT (Christensen and Aubert, 2006) to 4. mT (Starchenko and Jones, 2002). Using $E_M = 4. \times 10^{-9}$ yields S of the order of $10^4 - 5. \times 10^4$.

3   Axisymmetric motions spawned in a spherical cavity by a sudden impulse of the spin of the inner core

The change of the relative strengths of the magnetic and rotation forces according to frequency is well illustrated by the contrast between transient and steady flows in a differentially rotating spherical shell in the presence of a magnetic field. Static solutions have been published in the case of dipolar magnetic field and small differential rotation, for which the structure of the flow has been described according to the Elsasser number (Hollerbach, 1994; Dormy et al., 1998). Kleeorin et al. (1997) have theoretically investigated steady linear solutions when the imposed magnetic field is potential and has dipole parity. They have identified several asymptotic regimes according to values of the Elsasser number in the small Ekman number limit. Let us now study transient structures.

4

3.1 Model and governing equations

Consider an electrically conducting homogeneous fluid occupying a spherical shell that is immersed in an imposed steady magnetic field. The ratio of the inner shell radius b to the outer radius a is $b/a = 0.35$ as in the Earth's core. The solid inner core has the same electrical conductivity as the fluid and the outer boundary is insulating. The fluid is rotating with the constant angular velocity Ω. The imposed magnetic field is chosen as:

$$\mathbf{B} = B_0 \nabla \times (A\mathbf{e}_\phi) \tag{7}$$
$$A = (j_1(\beta_{11}r) - 0.3j_1(\beta_{12}r))P_1^1(\cos\theta) - 0.2\,j_3(\beta_{31}r)P_3^1(\cos\theta) \tag{8}$$

where (r, θ, ϕ) are spherical coordinates, P_l^1 are Legendre functions, $(j_l)_l$ is the set of spherical Bessel functions of the first kind and β_{ln} is the nth root of $j_{l-1}(\beta) = 0$. The basic field, which is shown in figure 1, has been chosen with the aim of modelling torsional oscillations in the Earth's fluid core. In this context, the important quantity (Braginsky, 1970) is

$$\{B_s^2\}(s) = \frac{1}{2\pi(z_T - z_B)} \left(\oint \int_{z_B}^{z_T} B_s^2 dz d\phi \right), \tag{9}$$

evaluated on geostrophic cylinders of radius s and of top and bottom z-coordinates respectively z_T and z_B. Obviously, the choice (8) is arbitrary. In contrast with the Earth's case and with the basic state used by Braginsky (1980) to model torsional oscillations, $\{B_s^2\}$ vanishes at $s = a$ because of the imposed dipole symmetry with respect to the equatorial plane. Axisymmetry makes $\{B_s^2\} = 0$ at $s = 0$ in contrast with the geophysical case again. In view of the present study, the main characteristics of the field $\mathbf{B}$ defined by (8) are that it is neither parallel to the rotation axis nor rapidly decreasing with radius as are current-free dipole fields. The results presented below do not depend on the details of the geometry of $\mathbf{B}$.

Study the evolution of the velocity field $\mathbf{u}$ and of the magnetic field deviation $\mathbf{b}$ after an impulsive increase of the angular rotation ω_b of the inner core, postulating symmetry about the axis of rotation and dipole symmetry about the equatorial plane:

$$
\begin{aligned}
u_r(r, \pi - \theta, \phi) &= u_r(r, \theta, \phi), & u_\theta(r, \pi - \theta, \phi) &= -u_\theta(r, \theta, \phi), \\
u_\phi(r, \pi - \theta, \phi) &= u_\phi(r, \theta, \phi), & b_r(r, \pi - \theta, \phi) &= -b_r(r, \theta, \phi), \\
b_\theta(r, \pi - \theta, \phi) &= b_\theta(r, \theta, \phi), & b_\phi(r, \pi - \theta, \phi) &= -b_\phi(r, \theta, \phi).
\end{aligned}
\tag{10}
$$

The amplitude of the initial impulse Ω_b is assumed to be small enough so that the subsequent evolution of the dynamics is independent of Ω_b within a scaling factor. Using B_0 as unit of magnetic field, a as length-scale and $a(\mu\rho)^{1/2}/B_0$ as unit of time, the fields $\mathbf{u}$ and $\mathbf{b}$ are governed by the following linearised equations in the fluid region:

$$\frac{\partial \mathbf{u}}{\partial t} + 2\lambda^{-1}\mathbf{e_z} \times \mathbf{u} = -\nabla p + (\nabla \times \mathbf{B}) \times \mathbf{b} + (\nabla \times \mathbf{b}) \times \mathbf{B}$$
$$+ P_m \lambda \, \Lambda^{-1} \nabla^2 \mathbf{u}, \tag{11}$$

$$\frac{\partial \mathbf{b}}{\partial t} = \nabla \times (\mathbf{u} \times \mathbf{B}) + \lambda \, \Lambda^{-1} \nabla^2 \mathbf{b}, \tag{12}$$

where $P_m = \nu/\eta$ is the magnetic Prandtl number. The field $\mathbf{b}$ is defined also in the inner solid region where:

$$\frac{\partial \mathbf{b}}{\partial t} = \lambda \, \Lambda^{-1} \nabla^2 \mathbf{b}. \tag{13}$$

Note that the steady-state solutions depend only on the two parameters Λ and E. The velocity boundary conditions

$$\mathbf{u} = 0, \quad r = a \tag{14}$$
$$\mathbf{u} = s\, \omega_b(t) = s\, \Omega_b\, \delta(t - t_0), \quad r = b \tag{15}$$

are written using the Dirac δ function and are appropriate to rigid boundaries.

The set of equations (11) and (12) is discretized and time-stepped from an initial state of rest:

$$\mathbf{u} = \mathbf{b} = \mathbf{0} \tag{16}$$

The Dirac δ function is approached as:

$$\frac{1}{\sqrt{\pi\epsilon}} e^{-(t-t_0)^2/\epsilon}. \tag{17}$$

It is a result of the simulations below that the solutions are independent of the parameter ϵ provided that its value is set small enough.

A poloidal/toroidal decomposition

$$\mathbf{u} = u_\phi \mathbf{e}_\phi + \nabla \times (u_p \mathbf{e}_\phi) \tag{18}$$
$$\mathbf{b} = b_\phi \mathbf{e}_\phi + \nabla \times (b_p \mathbf{e}_\phi) \tag{19}$$
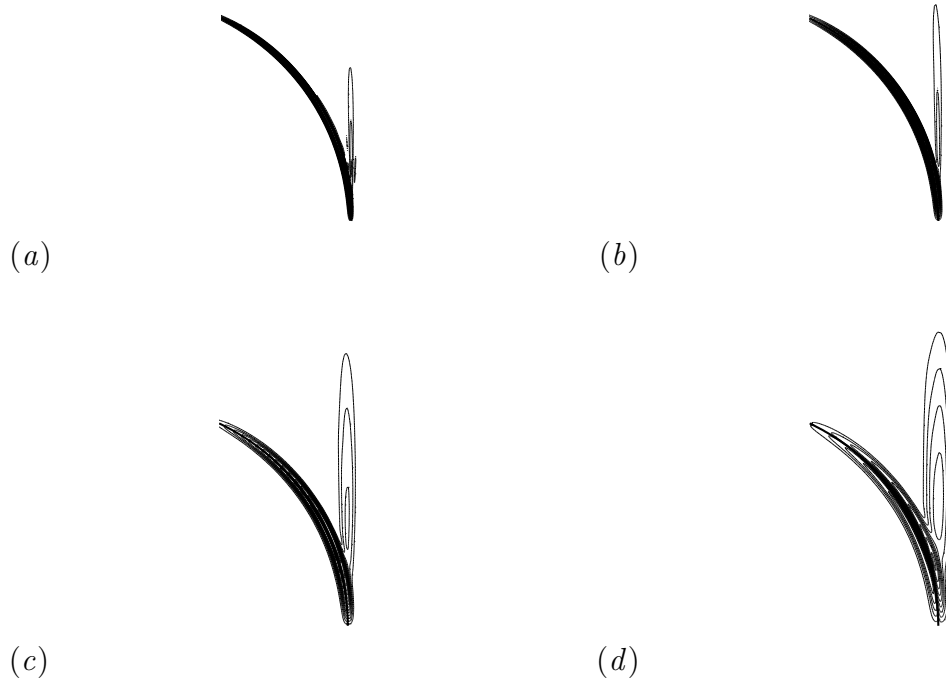
(a)

(b)

(c)

(d)

Figure 2. Contours of the induced azimutal magnetic field for $\lambda = 1.72 \times 10^{-4}$, $\Lambda = 0.52$, $E = E_M = 5.7 \times 10^{-8}$ drawn at $t = 8.6 \times 10^{-3}$(a), $t = 1.72 \times 10^{-2}$(b), $t = 3.44 \times 10^{-2}$(c) and $t = 6.88 \times 10^{-2}$(d). The contour intervals and the frame size are identical in all frames. The inner sphere boundary is indicated with a thick line.

is employed. The variables are expanded in associated Legendre functions, i.e.

$$u_\phi(s, \theta) = \sum_{l=0}^{lmax} u_\phi^l(s) P_{2l+1}^1(\cos \theta) \tag{20}$$

and then discretized in radius. The minimum truncation level $lmax$ is 120 whereas at least 450 unevenly spaced points are used in the radial direction.

3.2 Formation and propagation of geostrophic jets

Let us examine a typical sequence of solutions for a small value of λ. Following the initial impulse, an almost geostrophic shear sets up, after a few revolutions, at the cylindrical surface tangent to the inner core, hereafter referred to as tangent cylinder. Induction of an azimutal magnetic field localized at the tangent cylinder (compare the snapshot (a) to the snapshot (b) in figure 2 occurs about the end of this period during which the velocity field becomes axially invariant. It starts from a source at the equator of the inner core. The last two
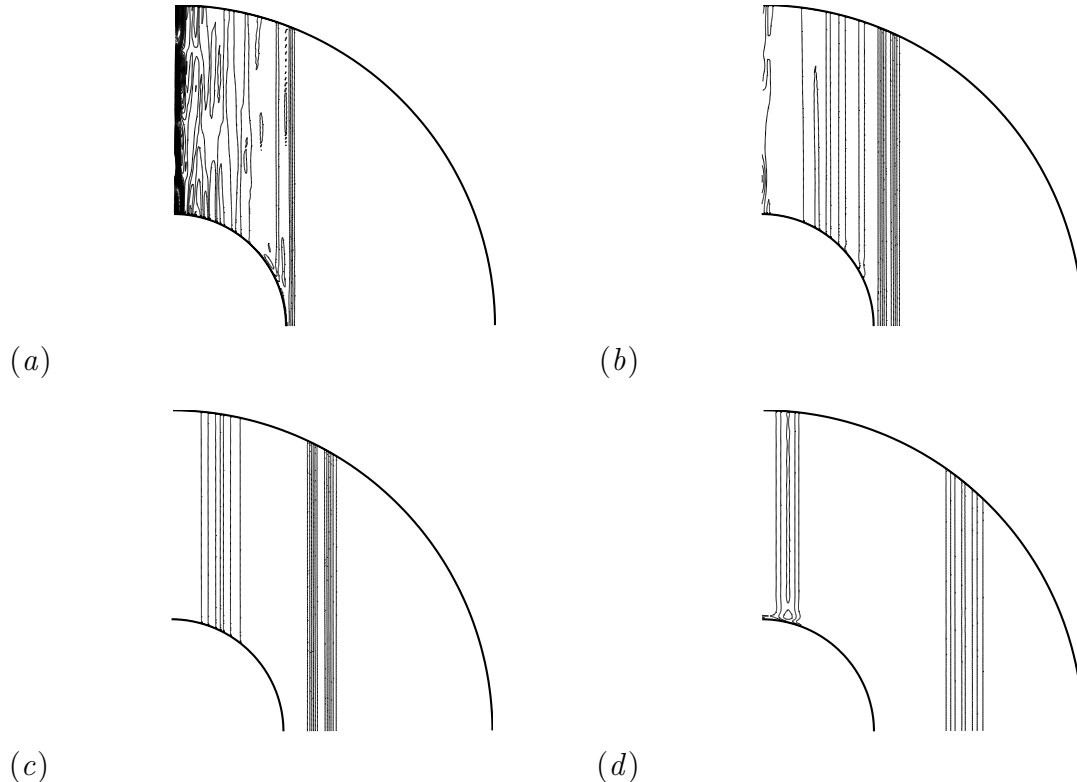
(a) (b)

(c) (d)

Figure 3. Contours of constant angular velocity for $\lambda = 1.72 \times 10^{-4}$, $\Lambda = 0.52$, $E = E_M = 5.7 \times 10^{-8}$ drawn at $t = 8.6 \times 10^{-2}$(a), $t = 0.26$(b), $t = 0.52$(c) and $t = 1.03$(d). The contour intervals are respectively $\Delta\omega$, $\Delta\omega/2$, $\Delta\omega/5$ and $\Delta\omega/10$ in the frames a, b, c and d in order to compensate for the attenuation of the velocities.

panels of figure 2 illustrates the following period during which meridional electrical currents parallel to the tangent cylinder intensify and loop further and further away from the tangent cylinder. This is the most noticeable feature before the geostrophic shear splits up. The outer shear readily transforms into a jet propagating away from the tangent cylinder towards larger cylindrical radii. Thereafter, the velocity within the jet becomes more and more invariant along z as time elapses (figure 3). On the other side of the tangent cylinder, a second shear propagates towards the axis of rotation. Its propagation velocity slows down as B_s decreases to 0 on the axis. In the event, the inner shear transforms also into a jet. The comparison (figure 4) with a second sequence of solutions for the same value of λ but for Λ multiplied by a factor of 12.5 indicates that the dynamics outside the tangent cylinder is almost independent of Λ. The flow remains geostrophic even though Λ is $O(1)$. Note that steady flows do not reproduce this feature. Figure 5 shows zonal flows driven by rotating the inner sphere at a constant rate for the two values of Λ used to calculate the transient solutions. For the largest value of Λ, the angular velocity contours are not parallel to the rotation axis and tend instead to follow the magnetic field lines, as prescribed by Ferraro's law of isorotation. Steady solutions are established after a period lasting a few time units $\lambda^{-1}\Omega^{-1}$ during
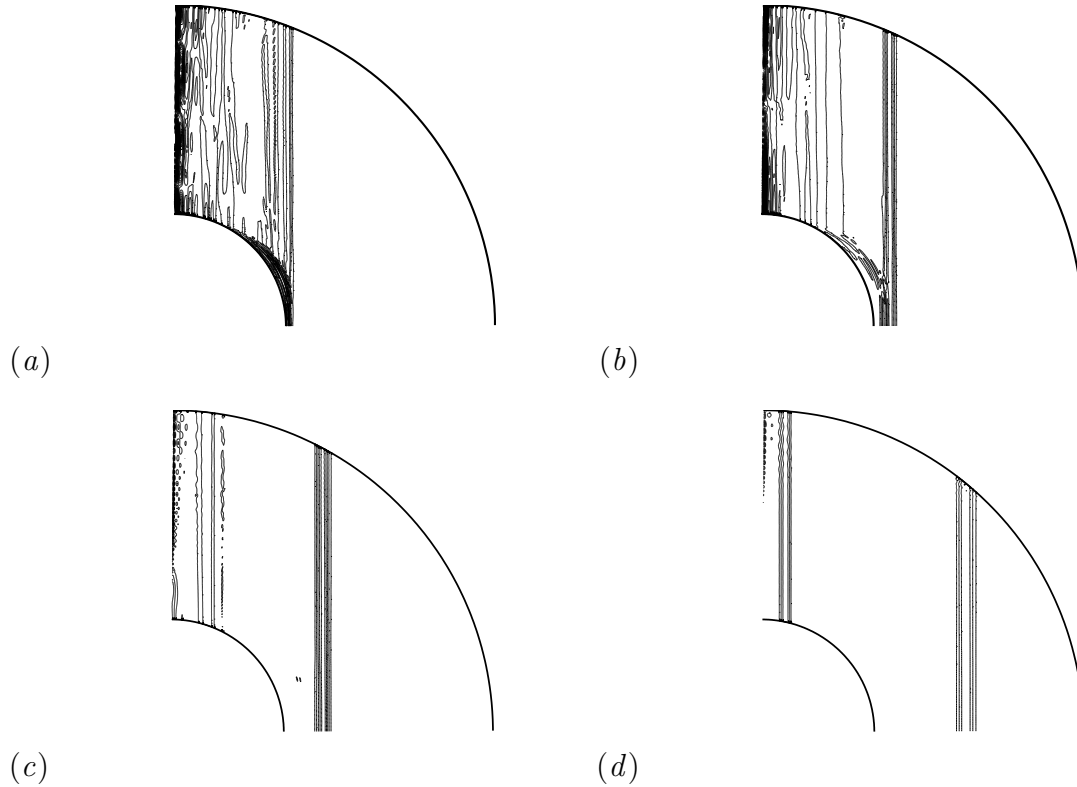
8

(a)   (b)

(c)   (d)

Figure 4. Same as figure 3 for $\lambda = 1.72 \times 10^{-4}$, $\Lambda = 6.5$, $E = 1.42 \times 10^{-8}$, $E_M = 4.5 \times 10^{-9}$ and same progression of contour intervals.
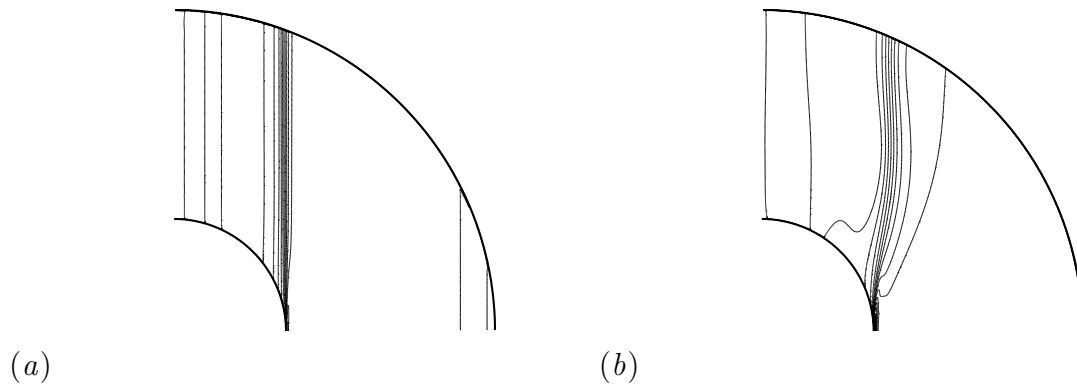

(a)   (b)

Figure 5. Steady azimuthal flow induced by rotating the inner and outer boundaries at slightly different rates. Contours of constant angular velocity for $E = 4.5 \times 10^{-7}$ and $\Lambda = 0.52$ (a) $\Lambda = 6.5$ (b).

which the flow is geostrophic.

The outer geostrophic jet has finite width δ in the limit $\epsilon \to 0$ (see expression (17) for the definition of ϵ). Investigating the variation of δ with λ, E, and E_M gives an useful insight into the mechanism of generation of the geostrophic motions. Here δ is arbitrarily defined as the distance along s between the two
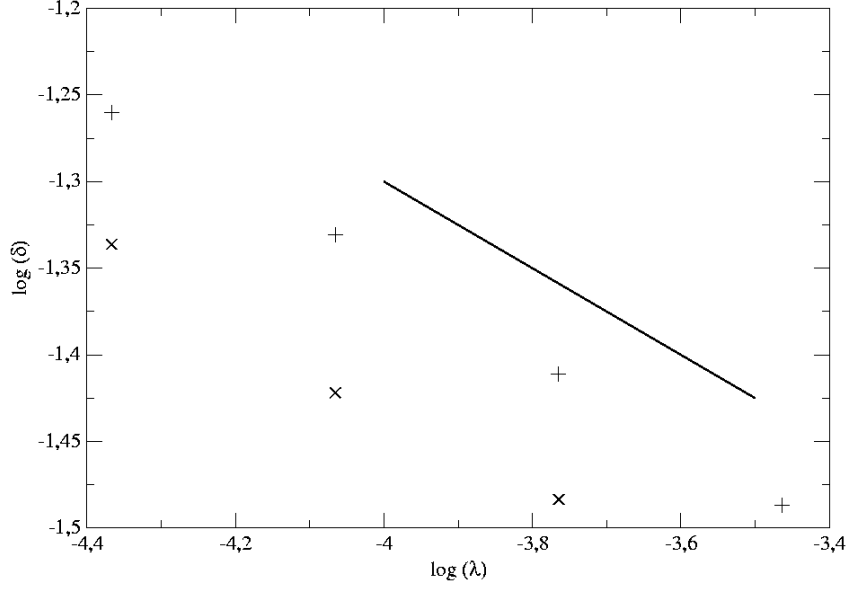
9

Figure 6. Scaling of the width δ of the outer geostrophic jet with respect to the number λ. The magnetic Prandtl number is $P_m = 1$ and the Ekman number is $E = 5.7 \times 10^{-8}$ (crosses) or $E = 2.85 \times 10^{-8}$ (+ signs). A line of slope $-1/4$ is shown for comparison.
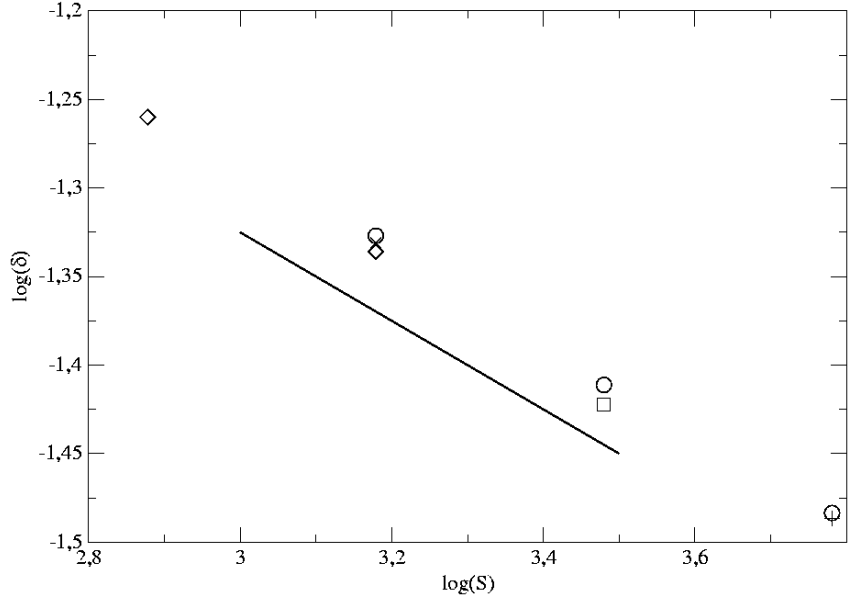

Figure 7. Scaling of the width δ of the outer geostrophic jet with respect to the Lundquist number $S^\dagger = \lambda/E_M$. The magnetic Prandtl number is $P_m = 1$ and λ is 4.3×10^{-5} ($\diamond$), 8.6×10^{-5} ($\times$), 1.72×10^{-4} ($\circ$), 3.44×10^{-4} (+), 6.88×10^{-4} ($\square$). A line of slope $-1/4$ is shown for comparison.

cylinders, on both sides of the geostrophic jet, where the angular velocity has half its maximum value. For the range of parameters that has been extensively explored, the outer layer is always well characterized from $t = 0.17$ onwards. Results are reported for this time. Keeping E constant and $P_m = 1$, it is found
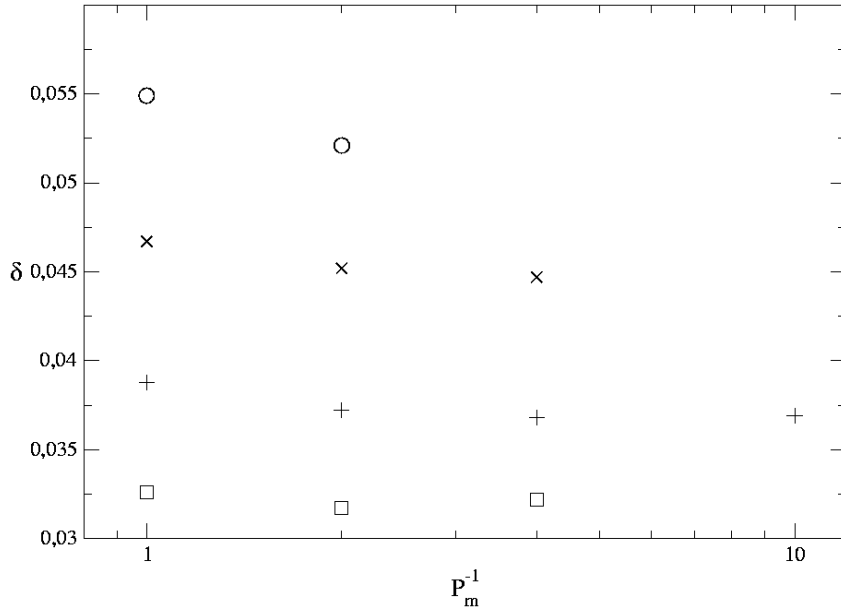
10

Figure 8. Thickness δ of the outer geostrophic jet with respect to P_m^{-1} for $P_m \leq 1$. and various λ: $\lambda = 4.3 \times 10^{-5}$ (circles), $\lambda = 8.6 \times 10^{-5}$ (crosses), $\lambda = 1.72 \times 10^{-4}$ (+ signs), $\lambda = 3.44 \times 10^{-4}$ (squares).

that δ varies as $\lambda^{-1/4}$ (see figure 6). For fixed values of λ and $P_m = 1$, δ varies as $E_M^{1/4}$. This is illustrated by the figure 7. Indeed, assuming $\delta \sim \lambda^{-1/4}$, the power law $\delta \sim E_M^{1/4}$ can simply be written:

$$\delta \sim \left(S^\dagger \right)^{-1/4} \tag{21}$$

using the Lundquist number $S^\dagger = \lambda (E_M)^{-1}$. Thus, the width δ is independent of the angular velocity Ω. We are interested by results for $P_m < 1$ since $\nu \ll \eta$ in the geophysical case and in laboratory experiments as well. Decreasing P_m from $P_m = 1$, a slight dependence of δ on P_m is found (figure 8). Extension of the relationship (21) to solutions for $P_m < 1$ is supported by these results.

The outer geostrophic jet is radiated from the tangent cylinder, which touches the inner core on its equatorial circle. There, both the rotation vector and the magnetic field are parallel to the inner core surface and the Ekman-Hartmann viscous boundary layer adjacent to the inner core is singular. Thus, it is instructive to investigate the influence of the strength of the magnetic field at the singularity. For this purpose, an axial uniform field can be added to the magnetic field defined by (8). It is found that the jet is much thickened if the two fields cancel out at the singularity. Then, the relationship (21) does not hold. On the other hand, it is also found - in the narrow parameter range which has been investigated - that the layer shrinks as $[B_z(b, 0)]^{-1/4}$ as the axial magnetic field adjacent to the equatorial ring of the inner core is increased. Taking this result at its face value, the magnetic field strength entering the

relationship (21) would be $B_z(b, 0)$. Putting these results together, it appears that the magnetic structure adjacent to the equator of the inner core plays a significant role in the emergence of the two propagating shear layers. The transformation of the outer shear layer into an independent jet detached from the inner core is promoted by the axial magnetic field.

Once the outer jet is formed, its time evolution is given by the equations of Braginsky (1970), which satisfy angular momentum conservation. It is possible to estimate the angular momentum $A(t) = s^2\sqrt{1 - s^2}\delta u_\phi(s)$ carried by the outer jet from the width δ. For the solutions that have been investigated, A does not change throughout the propagation of the jet. The strength B_s of the magnetic field sheared by the jet decreases with s to 0 at $s = 1$. Thus, the jet slows down as it approaches the outer sphere equator, which it never reachs.

The scaling (21) has implications for the coupling between the axial rotation of the Earth's solid inner core and torsional oscillations (Buffett and Mound, 2005). The time unit $\lambda^{-1}\Omega^{-1}$ corresponds to 1-10 years for geophysical applications. A characteristic time $\left(S^\dagger\right)^{-1/4}(\lambda\Omega)^{-1}$ can be derived from the length δ and the Alfvén wave velocity $\lambda\Omega a$. It corresponds to the inner core rotation period below which dissipative processes at the tangent cylinder are important. Using a geophysical estimate for $S^\dagger$, the coupling mechanism presented above between the rotation of the inner core and torsional Alfvén waves is found to be efficient on periods longer than a few months. Investigation of magnetic fields with non-dipole symmetry will be a natural follow-up of this study.

Finally, keeping $S^\dagger$ constant and increasing λ, it is found that the structures radiated from the tangent cylinder lose their geostrophic character for $\lambda \sim 10^{-2}$.

4 Discussion

Let us now examine to what extent the parameter λ is also appropriate to comment on the geometry of fast motions in other problems characterized by rapid rotation and magnetic field.

4.1 Axially invariant hydromagnetic instabilities occurring at small Lehnert number

We can discriminate between two approaches that have been followed to study the stability of a magnetic field in a rotating sphere according to the param-

eter, either λ or Λ, used to compare magnetic and rotation forces. Malkus (1967) recently followed by Zhang et al. (2003) studied hydromagnetic waves in a non-dissipative fluid ($\Lambda \rightarrow \infty$). As a result, they wrote the condition for stability as a relationship involving the Lehnert number λ, which has to exceed values of the order unity. Zhang and Fearn (1994) focused on the rapid rotation limit ($\lambda \rightarrow 0$) instead. Then, the onset of instability occurs for a critical value of the Elsasser number Λ_c. In accordance with the above discussion on the geometry of the motions in the limit ($\lambda \rightarrow 0$), they found that the (non-axisymmetric) instability is characterized by nearly two-dimensional columnar fluid motions despite Λ_c being $O(10)$.

This result stands when the instabilities are thermally driven. Zhang (1995) focused his study of rotating convection in the presence of an axisymmetrical toroidal magnetic field on the limit ($E \rightarrow 0$), which amounts to ($\lambda \rightarrow 0$) for finite values of the Elsasser number Λ. The magnetic Prandtl number is set to 1 and the control parameters are thus Λ together with a Rayleigh number. The fluid motions, in the limit ($E \rightarrow 0$), are almost two-dimensional showing only slight variations along the direction of the rotation axis whilst Λ is $O(1-10)$. The solutions of Olson and Glatzmaier (1995) (outside the cylindrical surface tangent to the inner core), Walker and Barenghi (1997) (their figures 6f, 7f, 8f, 9f) for different basic states and Zhang and Jones (1996) (their figure 4) for $\kappa/\eta \ll 1$, where κ is thermal diffusivity, all present similar features.

4.2 Columnar flow structure in geodynamo models

Obviously, the numbers λ and Λ are less directly relevant to studies of dynamo simulations than to investigations of models with imposed large-scale magnetic field. These two estimates of the magnetic field strength come out as output of the numerical runs instead of being among the initial parameters. It is nevertheless true that realistic values of λ are reached in numerical models of the geodynamo as λ does not involve diffusivities. Thus, Christensen and Aubert (2006) conducted a statistical analysis of a set of geodynamo models and estimated a parameter defined as λ, using the shell depth as the length-scale l in (3). Their results correspond to λ varying from 7×10^{-3} to 3×10^{-2}, keeping the core radius as length-scale. Christensen and Aubert (2006) found that the narrow range of λ values contrasts with the wide variations of Λ. They also remarked that measuring the relative strength of magnetic and rotation forces acting in geodynamo models with the Elsasser number Λ does not reflect the fact that the Lorentz force depends on the length scale of the magnetic field whereas the Coriolis force is independent of the length scale of the velocity field. Conversely, comparing typical periods of the Alfven waves to typical periods of the inertial waves shows that the relative importance of the magnetic force augments with decreasing length scales (see the expression (3)

of λ). In their previous systematical parameter study, Christensen et al. (1999) had found only one case with strong deviations from columnarity ($\Lambda = 14$, $E_M = 6 \times 10^{-5}$, $\lambda = 3 \times 10^{-2}$). Together, these results are consistent with the statement that the extent to which rotation affects the structure of the flow depends on λ, the motions remaining columnar up to $\lambda = O(3 \times 10^{-2})$.

4.3   Torsional oscillations in convective dynamo models

Convection columns can excite time-dependent geostrophic motions in dynamo models through magnetic and Reynolds stresses. This has been illustrated by Dumberry and Bloxham (2003). They separated the axisymmetric azimutal velocity field obtained from the geodynamo model of Kuang and Bloxham (1999) - $E = E_M = 4 \times 10^{-5}$, $P_r = 1$ and stress-free boundary conditions - into a mean flow plus a fluctuating component. They showed that the quasi-static azimutal winds have large gradients in the z-direction. On the other hand, Dumberry and Bloxham (2003) emphasized the axial invariance of the time-varying zonal flows. Their finding that, outside the tangent cylinder, the whole length of the geostrophic cylinders accelerates azimutally as if they were rigid on time-scales $\tau \sim 0.1\,\tau_D$ is in line with the small value of λ in this numerical experiment (τ_D magnetic diffusion time). Indeed, using $B \sim 2(2\Omega\mu\rho\eta)^{1/2}$ (see fig. 10 of Kuang and Bloxham (1999)), we infer $\Lambda \sim 10$ and $\lambda \sim 2 \times 10^{-2}$. These geostrophic motions are not Alfvén waves as Reynolds stresses and viscous forces are as important as the magnetic forces in the balance of forces acting on the geostrophic cylinders. More recently and with Earth-like no-slip boundary conditions, Takahashi et al. (2005) argued indeed that the Ekman number has to be decreased down to $E = 8 \times 10^{-6}$ to make the viscous torque acting on the geostrophic cylinders negligible and the magnetic torque predominant. Finally, for the same value of E as Takahashi et al. (2005), but with stress-free boundary conditions and small Prandtl number $P_r = 0.1$, Busse and Simitev (2005) found a dynamical state where the magnetic torques on geostrophic cylinders account for most of the geostrophic acceleration. Extracting the average magnetic field strength from the figure 18 of Busse and Simitev (2005) gives $\lambda \sim 5 \times 10^{-3}$ - well in the domain $\lambda \ll 1$ - and $\Lambda \sim 3$. The result that magnetic forces dominate over Reynolds stresses in the balance of force acting on the geostrophic cylinders can be related to the observation that the magnetic energy is much stronger than the kinetic energy in this solution. Thus, sequences where geostrophic motions behave as torsional oscillations begin to be detected in convective dynamo models. That requires $\lambda \ll 1$ - to obtain time-dependent geostrophic motions, observed for $\lambda \sim 2 \times 10^{-2}$ by Dumberry and Bloxham (2003) -, small E and, presumably, kinetic energy weaker than magnetic energy. In these studies, there is no evidence that the quantity $\{B_s^2\}$ measuring the intensity of the magnetic field sheared by the geostrophic motions and the geostrophic velocities evolve on

separate time-scales. Further work is needed to decide what kind of models (fully consistent dynamo models with poor separation of scales versus models incorporating a steady field) better describes the Earth's core dynamics.

4.4 Torsional oscillations and Taylor states

In this article, torsional oscillations are considered as part of the rapid motions that are dominated by rotation because magnetic diffusion is negligible. Braginsky (1970) had a different line of arguments. He attributed torsional oscillations to departures from a dynamic equilibrium where the net torque of the Lorentz force on any geostrophic cylinder is zero (Taylor, 1963). This condition has to be met, in spherical geometry, when only the Coriolis, pressure, buoyancy and magnetic forces are taken into account (MAC balance). It is frequently referred to as a "Taylor state". It describes a dynamo regime on the long time-scale for which magnetic diffusion is important. Reinstating the acceleration of geostrophic motions $\partial u_\phi(s)/\partial t$ in the equation for azimutal velocities, it has been possible to exhibit inviscid solutions of the model-Z of Braginsky (1978) that are in a Taylor state (Jault, 1995). However, this is almost the unique instance where a connection between torsional oscillations and idealized Taylor states has been vindicated. Geodynamo numerical models showing torsional oscillations that keep bringing back the magnetic field towards a Taylor state have not yet been found. The two viewpoints differ insofar nonzonal rapid motions are considered. I envision here that they are also constrained by rotation being almost z-invariant whereas Braginsky (1970) made no predictions on the geometry of these motions.

5 Concluding remarks

Focusing a numerical study on the transient motions spawned by an impulse in the rotation of the inner boundary of a rapidly rotating spherical shell immersed in a magnetic field with dipole symmetry, I have documented the emergence of geostrophic jets from the cylindrical surface that touches the inner core at its equator, irrespectively of the value of the Elsasser number. Both the poloidal motions, of which the vorticity is aligned along $\mathbf{e}_\phi$, and the toroidal motions with shear in the z direction are rapidly eliminated. The geostrophic layers travel with the velocity $\lambda a\Omega$ and are governed, outside the tangent cylinder, by the equations written by Braginsky (1970). The jet width scales as $\left(S^\dagger\right)^{-1/4}$. This estimate yields the frequency below which oscillations of the solid core are communicated to torsional Alfvén waves in the fluid shell. Using Earth-like parameters, it corresponds to a period of a few months. This study gives an illustration of the key role played - for fast flows - by the

parameter λ - independent of magnetic diffusivity - put forward by Lehnert (1954). Conversely, λ is not appropriate to study steady solutions as it cannot be derived from the two parameters Λ and E that characterize the static problem.

In the same spirit, I have been able to base a discussion of earlier numerical studies of magnetic instabilities and dynamos in rotating shells on that parameter λ. I suggest that the smallness of λ in some of these studies is the reason for the occurrence of columnar motions aligned parallel to the axis of rotation and also of geostrophic flows evolving as Alfvén waves. From these earlier studies, I anticipate that the results presented here can be extended to the nonaxisymmetric case.

Thus, the parameter λ, instead of the Elsasser number Λ , is the appropriate parameter to compare magnetic and rotation forces when flows evolving on time-scales much shorter than the magnetic diffusion time are considered. As the value of λ appropriate to the Earth's fluid core is $O(10^{-4})$, I advocate that motions in the core interior with fast diffusionless time-scales are approximately z-independent and columnar with vorticity aligned parallel to the rotation axis. That paves the way for dynamical studies of the flows responsible for the secular variation of the Earth's magnetic field, generalizing to all fast motions what has already been achieved for the geostrophic, axially symmetric ones (Zatman and Bloxham, 1997).

References

Braginsky, S. I., 1970. Torsional magnetohydrodynamic vibrations in the Earth's core and variations in day length. Geomag. Aeron. 10, 1–8.

Braginsky, S. I., 1978. Nearly axially symmetric model of the hydromagnetic dynamo of the Earth. Geomag. Aeron. 18, 225–231.

Braginsky, S. I., 1980. Magnetic waves in the core of the Earth. Geophys. Astrophys. Fluid Dyn. 14, 189–208.

Buffett, B. A., Mound, J. E., 2005. A Green's function for the excitation of

torsional oscillations in the Earth's core. J. Geophys. Res. 110 (B08104), 10.1029/2004JB003495.

Busse, F., Simitev, R., 2005. Convection in rotating spherical shells and its dynamo states. In: Soward, A. M., Jones, C. A., Hughes, D. W., Weiss, N. O. (Eds.), Fluid dynamics and dynamos in astrophysics and geophysics. The Fluid Mechanics of Astrophysics and Geophysics. CRC Press, pp. 359–392.

Busse, F. H., 1975. A model of the geodynamo. Geophys. J. R. Astr. Soc. 42, 437–459.

Cardin, P., Brito, D., Jault, D., Nataf, H.-C., Masson, J. P., 2002. Towards a rapidly rotating liquid sodium dynamo experiment. Magnetohydrodynamics 38, 177–189.

Christensen, U., Aubert, J., 2006. Scaling properties of convection-driven dynamos in rotating spherical shells and application to planetary magnetic fields. Geophys. J. Int. 166, 97–114.

Christensen, U., Olson, P., Glatzmaier, G. A., 1999. Numerical modelling of the geodynamo: a systematic parameter study. Geophys. J. Int. 138, 393–409.

Dormy, E., Cardin, P., Jault, D., 1998. MHD flow in a slightly differentially rotating spherical shell, with conducting inner core, in a dipolar magnetic field. Earth and Planetary Science Letters 160, 15–30.

Dumberry, M., Bloxham, J., 2003. Torque balance, Taylor's constraint and torsional oscillations in a numerical model of the geodynamo. Phys. Earth Planet. Inter. 140, 29–51.

Elsasser, W. M., 1946. Induction effects in terrestrial magnetism. Part 2. the secular variation. Physical Review 70, 202–212.

Grote, E., Busse, F., 2001. Dynamics of convection and dynamos in rotating spherical fluid shells. Fluid Dynamics Research 28, 349–368.

Hollerbach, R., 1994. Magnetohydrodynamic Ekman and Stewartson layers in a rotating spherical shell. Proc. R. Soc. Lond. A 444, 333–346.

Hollerbach, R., Jones, C. A., 1993. Influence of the Earth's inner core on geomagnetic fluctuations and reversals. Nature 365, 541–543.

Jault, D., 1995. Model Z by computation and Taylor's condition. Geophys. Astrophys. Fluid Dyn. 79, 99–124.

Kleeorin, N., Rogachevskii, I., Ruzmaikin, A., Soward, A. M., Starchenko, S., 1997. Axisymmetric flow between differentially rotating spheres in a dipole field. J. Fluid Mech. 344, 213–244.

Kuang, W., Bloxham, J., 1999. Numerical modeling of magnetohydrodynamic convection in a rapidly rotating spherical shell: weak and strong field dynamo action. J. Comput. Phys. 153, 51–81.

Lehnert, B., 1954. Magnetohydrodynamic waves under the action of the Coriolis force. Astrophysical Journal 119, 647–654.

Malkus, W. V. R., 1967. Hydromagnetic planetary waves. J. Fluid Mech. 28, 793–802.

Olson, P., Christensen, U., Glatzmaier, G. A., 1999. Numerical modelling of the geodynamo: Mechanisms of field generation and equilibration. J. Geo-

phys. Res. 104 B5, 10383–10404.

Olson, P., Glatzmaier, G. A., 1995. Magnetoconvection in a rapidly rotating spherical shell: structure of flow in the outer core. Phys. Earth Planet. Inter. 92, 109–118.

Roberts, P. H., 1967. An introduction to magnetohydrodynamics. Elsevier, New York.

Starchenko, S., Jones, C. A., 2002. Typical velocities and magnetic field strengths in planetary interiors. Icarus 157, 426–435.

Takahashi, F., Matsushima, M., Honkura, Y., 2005. Simulations of a quasi-Taylor state geomagnetic field including polarity reversals on the Earth simulator. Science 309, 459–461.

Taylor, J. B., 1963. The magneto-hydrodynamics of a rotating fluid and the Earth's dynamo problem. Proc. R. Soc. Lond. A274, 274–283.

Walker, M. R., Barenghi, C. F., 1997. Magnetoconvection in a rapidly rotating sphere. Geophys. Astrophys. Fluid Dyn. 85, 129–162.

Zatman, S., Bloxham, J., 1997. Torsional oscillations and the magnetic field within the Earth's core. Nature 388, 760–763.

Zhang, K., 1995. Spherical shell rotating convection in the presence of a toroidal magnetic field. Proc. R. Soc. Lond. A 448, 245–268.

Zhang, K., Fearn, D. R., 1994. Hydromagnetic waves in rapidly rotating spherical shells generated by magnetic toroidal decay modes. Geophys. Astrophys. Fluid Dyn. 77, 133–157.

Zhang, K., Jones, C. A., 1996. On small roberts magnetoconvection in rapidly rotating systems. Proc. R. Soc. Lond. A 452, 982–995.

Zhang, K., Liao, X., Schubert, G., 2003. Nonaxisymmetric instabilities of a toroidal magnetic field in a rotating sphere. Astrophysical Journal 585, 1124–1137.